Molecular Plant Pathology

MOLECULAR PLANT PATHOLOGY (2013) **14**(8), 791–802 DOI: 10.1111/mpp.12050

Co-immunoprecipitation-based identification of putative BAX INHIBITOR-1-interacting proteins involved in cell death regulation and plant–powdery mildew interactions

CORINA WEIS[1], SEBASTIAN PFEILMEIER[1], ERICH GLAWISCHNIG[2], ERIKA ISONO[3], FIONA PACHL[4], HANNES HAHNE[4], BERNHARD KUSTER[4], RUTH EICHMANN[1,†] AND RALPH HÜCKELHOVEN[1,*]

[1]*Lehrstuhl für Phytopathologie, Technische Universität München, 85354 Freising, Germany*
[2]*Lehrstuhl für Genetik, Technische Universität München, 85354 Freising, Germany*
[3]*Lehrstuhl für Systembiologie der Pflanzen, Technische Universität München, 85354 Freising, Germany*
[4]*Lehrstuhl für Proteomik und Bioanalytik, Technische Universität München, 85354 Freising, Germany*

SUMMARY

The endoplasmic reticulum (ER)-resident BAX INHIBITOR-1 (BI-1) protein is one of a few cell death suppressors known to be conserved in animals and plants. The function of BI-1 proteins in response to various biotic and abiotic stress factors is well established. However, little is known about the underlying mechanisms. We conducted co-immunoprecipitation (co-IP) experiments to identify *Arabidopsis thaliana* BI-1-interacting proteins to obtain a potentially better understanding of how BI-1 functions during plant–pathogen interactions and as a suppressor of cell death. Liquid chromatography and tandem mass spectrometry (LC-MS/MS) identified 95 proteins co-immunoprecipitated with green fluorescing protein (GFP)-tagged BI-1. Five selected candidate proteins, a RIBOPHORIN II (RPN2) family protein, VACUOLAR ATP SYNTHASE SUBUNIT A (VHA-A), cytochrome P450 83A1 (CYP83A1), H^+-ATPASE 1 (AHA1) and PROHIBITIN 2 (PHB2), were further investigated with regard to their role in BI-1-associated processes. To this end, we analysed a set of *Arabidopsis* mutants in the interaction with the adapted powdery mildew fungus *Erysiphe cruciferarum* and on cell death-inducing treatments. Two independent *rpn2* knock-down mutants tended to better support powdery mildew, and a *phb2* mutant showed altered responses to cell death-inducing *Alternaria alternata* f.sp. *lycopersici* (AAL) toxin treatment. Two independent *cyp83a1* mutants showed a strong powdery mildew resistance phenotype and enhanced sensitivity to AAL toxin. Moreover, co-localization studies and fluorescence resonance energy transfer (FRET) experiments suggested a direct interaction of BI-1 with CYP83A1 at the ER.

**Correspondence*: Email: hueckelhoven@wzw.tum.de
†*Present address*: The School of Life Sciences, University of Warwick, Gibbet Hill Campus, Coventry CV4 7AL, UK.

INTRODUCTION

BAX INHIBITOR-1 (BI-1) was first identified as testis-enhanced gene transcript (TEGT) in mammals (Walter *et al*., 1994). In 1998, BI-1 was recovered in a functional screening for cDNA clones, rescuing yeast cells from mammalian BAX-induced cell death, and was consequently renamed (Xu and Reed, 1998). In the following year, Kawai *et al*. (1999) studied the first plant BI-1 homologues in rice and *Arabidopsis thaliana*. Although the cell death-activating BAX protein itself is apparently not present in plants, the overexpression of plant *BI-1* suppresses mammalian BAX-induced programmed cell death (PCD) in yeast and in plants (Eichmann *et al*., 2006; Kawai *et al*., 1999; Sanchez *et al*., 2000). *BI-1* overexpression also inhibits cell death induced by the application of hydrogen peroxide (H_2O_2) or salicylic acid (SA) in tobacco BY-2 cells (Kawai-Yamada *et al*., 2004). Moreover, Watanabe and Lam (2006) showed accelerated cell death reactions in two *BI-1* knock-out mutants after treatment with the fungal toxin fumonisin B1 (FB1) or heat stress. Therefore, a conserved function of BI-1 proteins as cell death suppressors has been proposed (Hückelhoven, 2004; Kawai *et al*., 1999; Kawai-Yamada *et al*., 2001, 2004).

BI-1 proteins are resident in the endoplasmic reticulum (ER) and are predicted to possess six to seven transmembrane domains (Bolduc *et al*., 2003; Hückelhoven, 2004; Kawai *et al*., 1999; Xu and Reed, 1998). The C-terminal tail of BI-1 seems to be essential for cell death inhibition (Kawai-Yamada *et al*., 2004). *In silico* analyses predict that the C-terminal part forms a coiled-coil structure and reaches into the cytosol (Bolduc *et al*., 2003; Carrara *et al*., 2012; Kawai-Yamada *et al*., 2004). The exact operation of BI-1 proteins in inhibiting PCD is not yet understood. However, it has been demonstrated that BI-1 is involved in the regulation of the Ca^{2+} homeostasis of the ER and suppresses ER stress-induced cell death reactions (Ishikawa *et al*., 2011; Robinson *et al*., 2011).

In addition to their role as cell death inhibitors, BI-1 proteins are involved in plant responses to abiotic and biotic stress, e.g. on pathogen infection (Hückelhoven, 2004; Sanchez *et al*., 2000; Watanabe and Lam, 2006). In general, plant BI-1 proteins appear to support susceptibility to biotrophic pathogens and to limit the

© 2013 BSPP AND JOHN WILEY & SONS LTD

success of necrotrophic pathogens (reviewed in Ishikawa *et al*., 2011). For instance, barley BI-1 is required for full susceptibility to the powdery mildew fungus *Blumeria graminis* f.sp. *hordei* (Eichmann *et al*., 2010), but, when overexpressed, limits susceptibility to cell death-inducing microbes, such as the necrotrophic fungi *Botrytis cinerea* and *Fusarium graminearum*, the mutualistic root endophyte *Piriformospora indica* and the rust fungus *Phakopsora pachyrhizi* (Babaeizad *et al*., 2009; Deshmukh *et al*., 2006; Höfle *et al*., 2009; Imani *et al*., 2006).

Little is known about BI-1-interacting proteins. In mammals, BI-1 has been shown to interact with the inositol-3-phosphate receptor (Kiviluoto *et al*., 2012), with a NADPH-P450 reductase and with the cytochrome p450 monooxygenase 2E1 (CYP2E1) (Kim *et al*., 2009). These interactions probably regulate metabolic activity or functions of the interaction partners in signal transduction (Robinson *et al*., 2011). BI-1 can also serve as a docking protein for actin, supporting actin polymerization during cell adhesion (Lee *et al*., 2010). In addition, BI-1 might be involved in pathogenesis as a direct target of effector proteins of pathogenic *Escherichia coli* (Hemrajani *et al*., 2010). In plants, Ihara-Ohori *et al*. (2007) demonstrated the interaction of the C-terminal region of *A. thaliana* BI-1 with the calcium-binding protein calmodulin. This interaction is crucial for the suppression of hypersensitive reaction (HR)-associated cell death induced by avirulent *Pseudomonas syringae* (Kawai-Yamada *et al*., 2009). Recently, BI-1 has also been described to interact with cytochrome b_5 in complexes with very-long-chain fatty acid hydroxylases, which are involved in sphingolipid biosynthesis and cell death suppression (Nagano *et al*., 2009, 2012).

In this study, we conducted a co-immunoprecipitation (co-IP) assay using BI-1-green fluorescing protein (GFP)-expressing *Arabidopsis* mutants in order to identify further BI-1-interacting proteins and to elucidate the physiological environment of BI-1. Of 95 identified BI-1-co-immunoprecipitated proteins, which were not present in the control samples, five selected candidate proteins were analysed further with regard to their impact on BI-1-associated processes. Direct interaction with BI-1 was independently confirmed for cytochrome P450 83A1 (CYP83A1). Furthermore, CYP83A1 was required for a compatible interaction of *Arabidopsis* with the adapted powdery mildew fungus *Erysiphe cruciferarum* and for cell death control.

RESULTS

Co-IP-based identification of putative BI-1-interacting proteins

In order to identify interaction partners of *Arabidopsis* BI-1, co-IP was performed using *BI-1-GFP*-expressing *Arabidopsis* mutants. Empty vector Bin19 mutants served as control plants (Kawai-Yamada *et al*., 2001). Both *Arabidopsis* mutants were either noninoculated or inoculated with adapted *E. cruciferarum* and nonadapted *B. graminis* f.sp. *hordei*, respectively. The total protein input for co-IP was extracted from a pool of all variants in order to gain as many putative BI-1-interacting proteins as possible. BI-1-GFP and putative interaction partners were co-immunoprecipitated using GFP-binding agarose beads and identified by liquid chromatography and tandem mass spectrometry (LC-MS/MS), in conjunction with database searching against the viridiplantae subset of the National Center for Biotechnology Information (NCBI) database.

A total of 127 proteins was identified in the BI-1-GFP sample, 95 of which were not present in the empty vector control sample. Table S1 (see Supporting Information) lists these 95 BI-1-GFP co-immunoprecipitated proteins. Cowling and Birnboim (1998) showed that human BI-1 can be resistant to trypsin proteolysis. This might explain the detection of only one BI-1 peptide (AHLGDMDYVK, position 201–212). However, Western blots against GFP showed a successful precipitation of BI-1-GFP (Fig. S1, see Supporting Information), and Mascot database search against the whole NCBI database revealed an enrichment of GFP peptides in the BI-1-GFP co-immunoprecipitate, again validating a successful precipitation of BI-1-GFP. For first examinations, five putatively membrane-associated BI-1-interacting candidates were selected, predominantly according to their presumed BI-1-associated function and predicted subcellular localization: RIBOPHORIN II (RPN2) family protein [syn. HAPLESS 6 (HAP6)], VACUOLAR ATP SYNTHASE SUBUNIT A (VHA-A), cytochrome P450 83A1 [CYP83A1, syn. REDUCED EPIDERMAL FLUORESCENCE 2 (REF2)], H^+-ATPASE 1 (AHA1) and PROHIBITIN 2 (PHB2) (Table 1). Candidates were selected after a quality check of the respective mass spectra by manual inspection, although not all identified peptides showed significant Mascot ion scores. The five selected putative BI-1-interacting proteins are listed in Table 1, including information about the Arabidopsis Genome Initiative (AGI) code, the amino acid sequence of the identified peptides, the Mascot ion score (threshold, 46; at $P < 0.05$) and the assumed subcellular localization, according to The Arabidopsis Information Resource (TAIR, http://arabidopsis.org) annotation. co-IP was repeated twice. RPN2, VHA-A, AHA1 and PHB2 co-immunoprecipitated with BI-1-GFP in all three independent experiments. CYP83A1 was identified in two independent repetitions.

According to TAIR, RPN2/HAP6 is predicted to have dolichyl-diphosphooligosaccharide-protein glycotransferase activity as part of the oligosaccharyltransferase (OST) complex catalysing the *N*-glycosylation of proteins in the ER (Kang *et al*., 2008; Liu and Howell, 2010). Correct *N*-glycosylation is critical for the prevention of ER stress, and Watanabe and Lam (2008) have shown a role of BI-1 in the suppression of ER stress. This might functionally link BI-1 and RPN2. V-ATPases can function in the trans-Golgi network and play essential roles in stress responses (Dettmer *et al*., 2005,

Table 1 Proteins that co-immunoprecipitated with BAX INHIBITOR-1 (BI-1), which were selected for further analyses.

Gene description†	AGI code	Identified peptides	Mascot ion score	Predicted localization‡
RIBOPHORIN II (RPN2) family protein§	At4g21150	(K)TLEILGIDKK(S)	38.96	CW, ER, M, Mit, Pl, PM, VM
		(K)VLQSSSSTLK(D)	**48.82***	
		(K)SVDSSVINNQELK(F)	38.24	
		(K)FDADSATYFLDSFPK(N)	**47.89***	
VACUOLAR ATP SYNTHASE SUBUNIT A (VHA-A)	At1g78900	(K)LAADTPLLTGQR(V)	44.6	Chlo, CW, M, Pl, PM, V, VM
		(R)LVSQKFEDPAEGEDTLVEK(F)	35.59	
		(R)TTLVANTSNMPVAAR(E)	**68.24***	
Cytochrome P450 83A1 (CYP83A1)¶	At4g13770	(K)LPPGPSPLPVIGNLLQLQK(L)	41.4	n.s.
H^+-ATPASE 1 (AHA1), AHA2	At2g18960 At4g30190	(R)EGLTTQEGEDR(I)	35.8	M, N, Pl, PM, V
PROHIBITIN 2 (PHB2)	At1g03860	(R)EIAQTIAQSANK(V)	**52.81***	Chlo, CW, Mit, P, V, VM

*Significant Mascot ion score at $P < 0.05$.

†Proteins were co-immunoprecipitated with BI-1-green fluorescing protein (GFP) and identified by liquid chromatography and tandem mass spectrometry (LC-MS/MS) in conjunction with database searching using Mascot. Selected candidate proteins are sorted by the number of identified peptides and alphabetically. Gene description and Arabidopsis Genome Initiative (AGI) code based on National Center for Biotechnology Information (NCBI) and The Arabidopsis Information Resource (TAIR) annotations, respectively.

‡Predicted protein localizations based on TAIR annotations and listed in alphabetical order. Chlo, chloroplast; CW, cell wall; ER, endoplasmic reticulum; M, membrane; Mit, mitochondria; N, nucleus; P, plastid; Pl, plasmodesmata; PM, plasma membrane; V, vacuole; VM, vacuolar membrane; n.s., not specified.

§TAIR annotation: HAPLESS 6 (HAP6).

¶Additional TAIR annotation: REDUCED EPIDERMAL FLUORESCENCE 2 (REF2).

2006; Dietz *et al*., 2001). Therefore, we chose the BI-1-GFP-co-immunoprecipitated VHA-A as a candidate protein. Recently, Keinath *et al*. (2010) have shown that the *AHA1* mutant *open stomata 2* is affected in immune signalling triggered by the perception of pathogen-associated molecular patterns (PAMPs). In barley, plasma membrane H^+-ATPases have been suggested to be involved in HR-mediated resistance to *B. graminis* f.sp. *hordei* (Finni *et al*., 2002; Zhou *et al*., 2000). However, the identified peptide (Table 1) is also part of AHA2. Another interesting candidate is PHB2. PHBs are involved in the prevention of stress responses and seem to play a major role in cell death-related mitochondrial function (Di *et al*., 2010; Van Aken *et al*., 2007, 2010). In human cells, BI-1 apparently regulates cell death by interaction with CYP2E1 (Kim *et al*., 2009), a homologue of CYP83A1, which we found to co-precipitate with BI-1-GFP. Interestingly, a search of the human CYP2E1 sequence against the *A. thaliana* database of NCBI identified CYP83A1 as the best hit (28% identity and 48% positives). Therefore, and because P450 monooxygenases are often associated with ER, we included CYP83A1 in further investigations.

Investigations on the function of putative BI-1-interacting proteins in response to *E. cruciferarum*

To analyse the function of BI-1-interacting candidate proteins in a plant–pathogen interaction, we conducted an assay using *Arabidopsis* mutants predicted to be deficient in the expression of *PHB2*, *RPN2*, *CYP83A1*, *AHA1* or *VHA-A*, which we inoculated with the adapted powdery mildew fungus *E. cruciferarum*.

We did not observe *PHB2* expression in the two independent *PHB2* mutants, *phb2-1* (SALK_004663C) and *phb2-2* (SALK_061282C), using reverse transcription-polymerase chain reaction (RT-PCR) (Fig. 1a). However, in *phb2-1*, the T-DNA insertion is in the promoter region, 850 bp upstream of the open reading frame (Fig. S2a, see Supporting Information). Therefore, we cannot exclude a residual expression of *PHB2* in this mutant. Microscopic analyses showed a slightly, but not significantly, increased fungal development on both *phb2* mutants, 5 days after inoculation (dai), measured as the number of conidiophores per colony (c/c). On the wild-type Col-0, the fungus developed an average number of about 20 c/c, whereas the conidiophore production was enhanced to 23 c/c and 25 c/c on *phb2-1* and *phb2-2*, respectively (Fig. 1a). At the macroscopic level, we did not observe obvious differences in symptom development on leaves of *phb2-1* and *phb2-2* when compared with Col-0 (not shown).

As *rpn2* loss of function hampers the growth of the pollen tube into the style, only heterozygous *rpn2* mutants can be obtained (Johnson *et al*., 2004). Both heterozygous *rpn2* mutants, *rpn2-1* (SALK_019955C) and *rpn2-2* (SALK_017994C), expressed *RPN2* at a clearly reduced level when compared with the wild-type (Fig. 1b). For the mutant *rpn2-2*, we cannot exclude an influence on the expression of At4g21140 (uncharacterized protein), as the T-DNA insertion is located in the common promoter region of *RPN2* (At4g21150) and At4g21140. Both *rpn2* mutants were similar, in that they supported a slightly increased fungal development when compared with the wild-type. The fungus developed 12 c/c on wild-type Col-0. On *rpn2-1* and *rpn2-2*, *E. cruciferarum* developed 17 c/c and 19 c/c, respectively (Fig. 1b). This effect was statistically significant for *rpn2-2*. At later points in time, leaves of *rpn2-1* and *rpn2-2* seemed to be only slightly more infected by powdery mildew than the wild-type, as assessed with the naked eye (not shown).

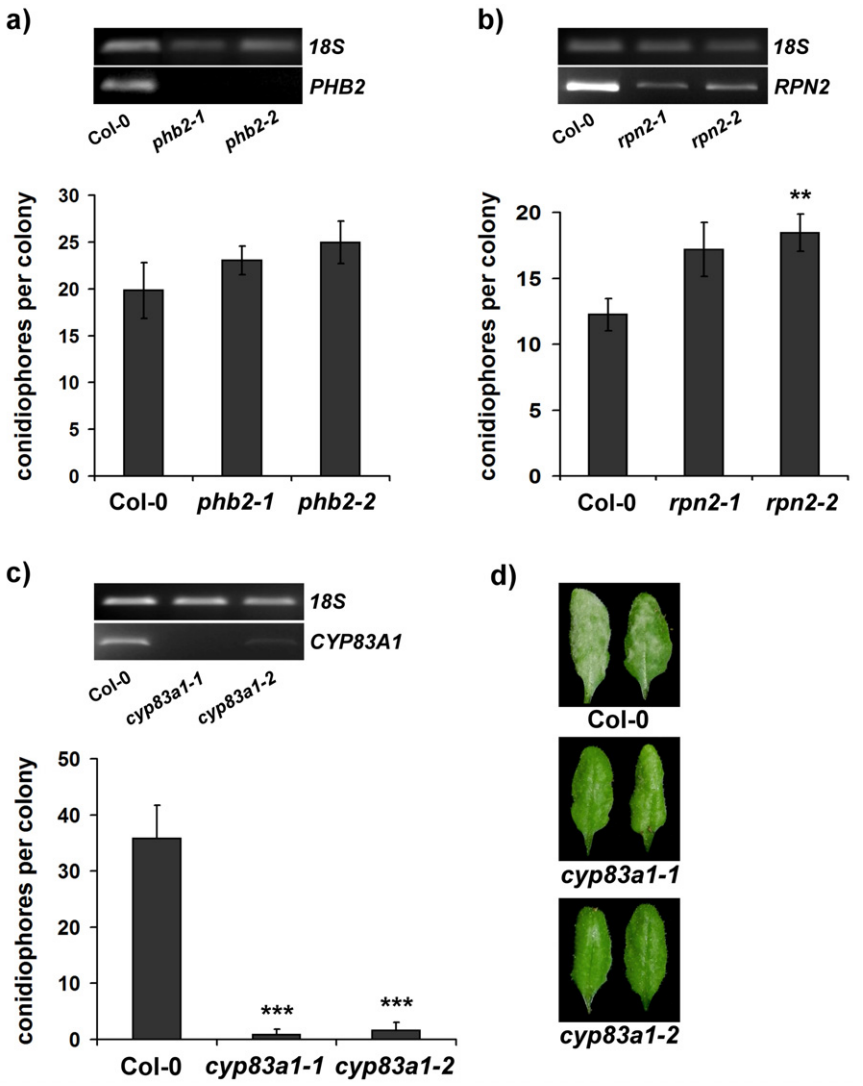

Fig. 1 *Erysiphe cruciferarum* development on *prohibitin* 2 (*phb2*), *ribophorin II* (*rpn2*) and *cytochrome P450 83A1* (*cyp83a1*) mutants. Plants of 5-week-old wild-type Col-0, *phb2-1* and *phb2-2* (a), wild-type Col-0, *rpn2-1* and *rpn2-2* (b) or wild-type Col-0, *cyp83a1-1* and *cyp83a1-2* (= *ref2-1*) (c) were inoculated with *E. cruciferarum* spores. Leaves were harvested at 5 days after inoculation (dai), and conidiophores per colony (c/c) were counted on five individual plants per line; 50 colonies per line were evaluated. Columns represent mean values. Bars represent standard errors. ** and *** indicate significance at $P < 0.01$ and $P < 0.001$, respectively, according to a two-sided unpaired Student's *t*-test calculated over the mean values of c/c on the single leaves. The experiment was repeated twice with similar results. In addition, reverse transcription-polymerase chain reaction products of *PHB2*, *RPN2* and *CYP83A1* analysed in Col-0 and the corresponding mutants are displayed. An *18S* fragment was amplified to confirm equal amounts of cDNA template. (d) Powdery mildew symptoms on Col-0, *cyp83a1-1* and *cyp83a1-2*. Five-week-old Col-0, *cyp83a1-1* and *cyp83a1-2* (= *ref2-1*) plants were inoculated with *E. cruciferarum* and photographed at 7 dai.

The T-DNA insertion mutant *cyp83a1-1* (SALK_123405C) did not express *CYP83A1* (Fig. 1c), and the loss-of-function point mutant *cyp83a1-2* (loss of function by premature stop codon), previously described as *ref2-1*, expressed a reduced amount of the mutant transcript (Fig. 1c and Hemm *et al*., 2003). The *cyp83a1* mutants stood out as a result of a dramatically reduced susceptibility to powdery mildew, which was readily visible with the naked eye (Fig. 1d). Concomitantly, the number of c/c was decreased strongly on both *cyp83a1* mutants compared with the wild-type at 5 dai. *Erysiphe cruciferarum* developed an average of 36 c/c on Col-0, and only 1 c/c and 2 c/c on *cyp83a1-1* and *cyp83a1-2*, respectively (Fig. 1c).

Hemm *et al*. (2003) demonstrated a reduced level of aliphatic glycosinolates and a slightly increased level of indole-derived glucosinolates in *cyp83a1-2* (= *ref2-1*). To investigate a pathogen-dependent influence on the glucosinolate composition, we measured the content of several glucosinolates in *cyp83a1-1* and Col-0 leaves at 5 dai with *E. cruciferarum* and in noninoculated control leaves. In noninoculated plants, the content of aliphatic glucosinolates was reduced in *cyp83a1-1* relative to wild-type plants, as described for *cyp83a1-2* (= *ref2-1*) (Hemm *et al*., 2003). However, under the conditions used, we observed only a marginally enhanced amount of indole-derived glucosinolates in *cyp83a1-1*. A pathogen-dependent influence on the glucosinolate content was hardly detectable. A tendency for induction by *E. cruciferarum* could be seen for 4-methoxy-indol-3-ylmethyl-glucosinolate at 5 dai in both genotypes (Fig. S3, see Supporting Information).

VHA-A T-DNA insertion lines (SALK_081473C, SALK_089595C) and an *AHA1* T-DNA insertion line (SALK_065288C) seemed to be as strongly infected by *E. cruciferarum* as Col-0 (data not shown), and were not further analysed in detail.

Overall, at least two of the five investigated BI-1-interacting candidate proteins appeared to have functions in the *Arabidopsis*–

E. cruciferarum interaction. Although RPN2 seems to limit fungal development, CYP83A1 is required for the susceptibility of *Arabidopsis* plants to *E. cruciferarum*.

Function of putative BI-1-interacting proteins in cell death reactions

To assess whether PHB2, RPN2 and CYP83A1 might be involved in BI-1-mediated cell death suppression, Col-0, *cyp83a1-1*, *cyp83a1-2* (= *ref2-1*), *phb2-2* and *rpn2-1* were treated with *Alternaria alternata* f.sp. *lycopersici* (AAL) toxin to induce cell death. The *BI-1* knock-out mutant *atbi1-2*, which showed enhanced sensitivity to the fungal toxin FB1 and to heat stress relative to wild-type plants (Watanabe and Lam, 2006), was included as a positive control. Cell death symptoms were evaluated 9–10 days after AAL toxin application. When compared with wild-type Col-0, AAL toxin-induced lesions were larger on *atbi1-2*, *cyp83a1-1*, *cyp83a1-2* and *phb2-2* (Fig. 2, for photographs see Fig. S4, Supporting Information). There was no altered sensitivity to AAL toxin application of *rpn2-1* mutant plants relative to Col-0 (Fig. 2). Control leaves treated with distilled water showed no cell death reactions at all. Thus, mutations of *CYP83A1* and *PHB2* also apparently alter *Arabidopsis* cell death responses. In a single experiment, seedlings of *atbi1-2*, *cyp83a1-1* and *phb2-2* also showed stronger cell death phenotypes after heat shock relative to Col-0. *rpn2-1* was slightly less affected after exposure to heat shock, when compared with Col-0 or *atbi1-2* (data not shown).

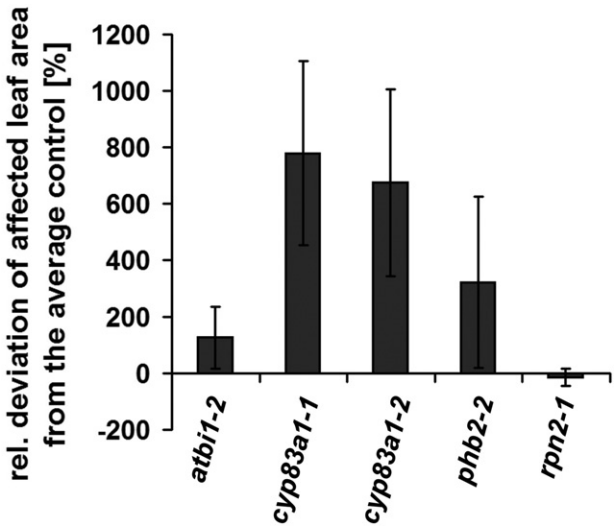

Fig. 2 Functional analysis of BAX INHIBITOR-1 (BI-1)-interacting candidate proteins in cell death reactions. Ten microlitres of a 100 μM *Alternaria alternata* f.sp. *lycopersici* (AAL) toxin solution were dropped on leaves of about 5-week-old Col-0, *atbi1-2*, *cyp83a1-1*, *cyp83a1-2*, *phb2-2* and *rpn2-1* plants. Leaves were evaluated 9–10 days after treatment. Per experiment, 10 leaves per line were used. The mean values of three or more totally independent experiments are displayed. Bars represent standard errors.

Co-localization of BI-1-GFP and fluorescence-labelled candidate proteins

Next, we performed co-localization studies of GFP-tagged BI-1 with red fluorescing protein (RFP)- or mCherry-tagged versions of CYP83A1, RPN2 or PHB2 in transiently transformed *Nicotiana tabacum* cv. Samsun leaf segments.

As already shown by Kawai-Yamada *et al*. (2001), BI-1-GFP localized in the ER and in the nuclear envelope (Fig. 3a). In control cells, soluble RFP served as a marker with localization in the cytoplasm and in the nucleus. Like mammalian prohibitins, *Arabidopsis* PHB2 is thought to be associated with mitochondria (Millar *et al*., 2001; Nijtmans *et al*., 2000). We confirmed the localization of PHB2 to mitochondria by the transient expression of PHB2-RFP in the marker line *mt-gk* (Nelson *et al*., 2007) (Fig. S5, see Supporting Information). As shown in Fig. 3a, PHB2-RFP accumulated in mitochondria all over the cell. Co-localization of BI-1-GFP and PHB2-RFP was visible in small dots, which presumably represent contact points of mitochondria with the ER and the nuclear envelope (Fig. 3a). We observed the same localization pattern after the transient transformation of *Arabidopsis* epidermal cells via particle bombardment (data not shown).

Cytochrome P450 proteins typically reside in the ER membrane (Schuler and Werck-Reichhart, 2003). As ER-localized CYP79F1 and CYP79F2 synthesize aliphatic aldoximes, which are substrates of CYP83A1, at the ER, CYP83A1 is also suggested to be present in this compartment (Chen *et al*., 2003; Nafisi *et al*., 2006; Reintanz *et al*., 2001). RPN2, as a dolichyl-diphosphooligosaccharide-protein glycotransferase, is also predicted to be present in the ER, where *N*-glycosylation takes place (Table 1). As predicted, CYP83A1-mCherry and RPN2-mCherry fusion proteins accumulated in the ER and around the nucleus in transiently transformed tobacco epidermal cells. Soluble GFP served as a co-transformed marker for cytosolic and nuclear localization (Fig. 3b,c). Co-expression of *BI-1-GFP* with either *CYP83A1-mCherry* or *RPN2-mCherry* resulted in overlapping fluorescence signals (Fig. 3b,c), confirming the accumulation of both putative BI-1-interacting proteins in the ER and around the nucleus. Comparative quantitative profiling of the fluorescence intensities of BI-1-GFP and either CYP83A1-mCherry or RPN2-mCherry further supported their co-localization (Fig. S6, see Supporting Information). The same localization patterns were observed in transiently transformed *Arabidopsis* epidermal cells after particle bombardment, but the fluorescence intensities were very low (not shown). Hence, RPN2 and CYP83A1 showed essential co-localization with BI-1, which supports the possibility of a physical protein–protein interaction.

BI-1 interacts with CYP83A1 at the ER

cyp83a1 mutants showed strong phenotypes in the interaction with *E. cruciferarum* and in cell death regulation. To test for a

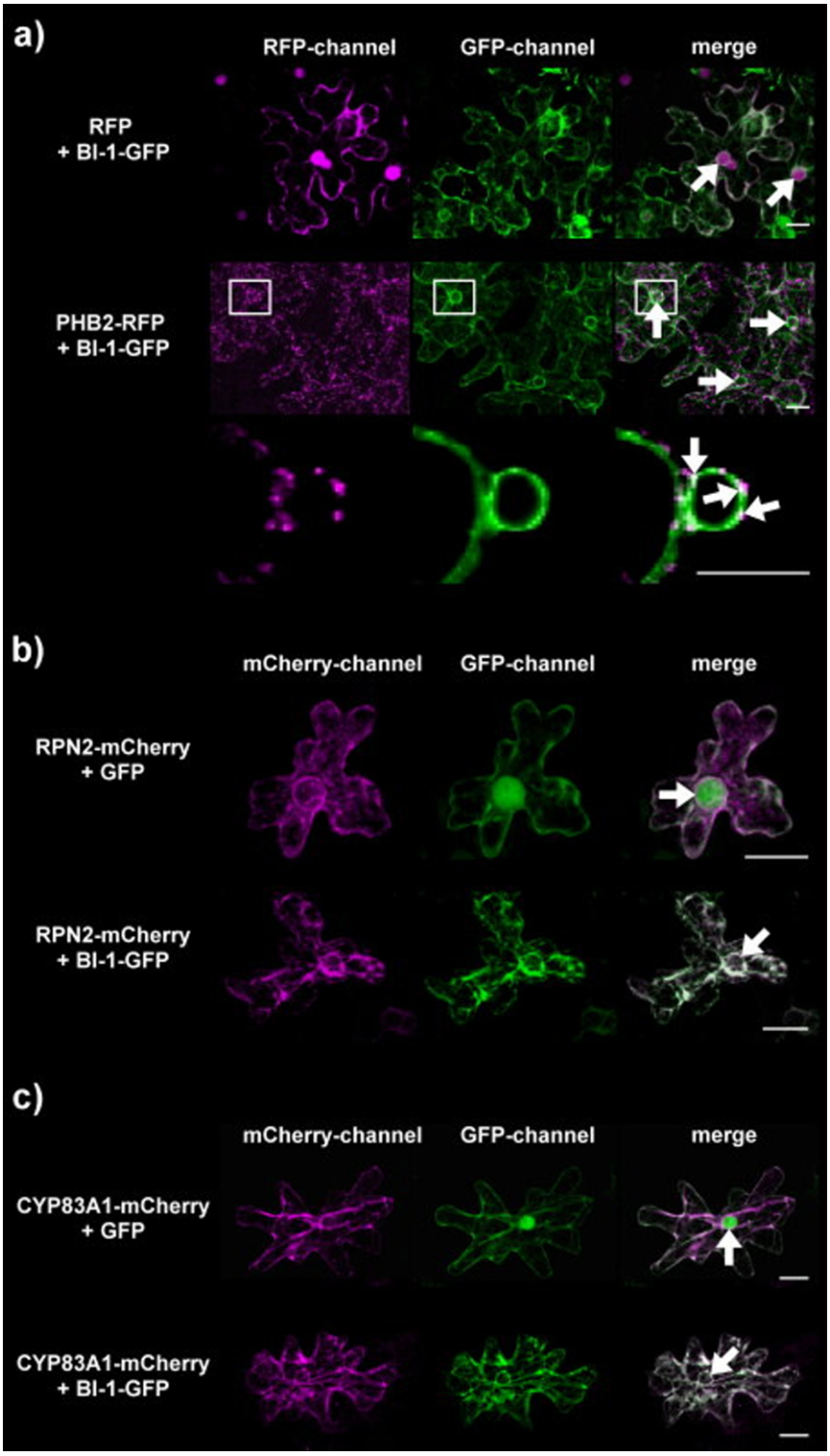

Fig. 3 Co-localization of BAX INHIBITOR-1-green fluorescing protein (BI-1-GFP) with PHB2-RFP, RPN2-mCherry or CYP83A1-mCherry in tobacco cells. (a) Tobacco epidermal cells transiently expressing BI-1-GFP together with RIBOPHORIN II (RFP) or PROHIBITIN 2-red fluorescing protein (PHB2-RFP) 5 days after *Agrobacterium tumefaciens*-mediated transformation. Soluble RFP served as a marker for cytoplasmic and nuclear localization. Fluorescence was visualized by confocal laser scanning microscopy (CLSM). The two top panels show whole-cell projections. The bottom panel shows the magnifications of the boxed areas in the panel above. Here, single sections are shown. (b, c) Tobacco leaf segments transiently expressing BI-1-GFP or GFP together with CYP83A1-mCherry or RPN2-mCherry, 6 and 3 days after *A. tumefaciens*-mediated transformation, respectively. Soluble GFP was co-expressed as a marker for cytoplasmic and nuclear localization. Fluorescence was visualized by CLSM. Photographs show whole-cell projections. (a–c) Arrows point to nuclei. White pixels in the merge image indicate overlapping fluorescence signals. Scale bars, 20 μm.

direct interaction between BI-1 and CYP83A1 at the ER, we conducted fluorescence resonance energy transfer (FRET) measurements by acceptor photobleaching using transiently transformed *Arabidopsis* epidermal cells. We chemically fixed the transformed leaves before the FRET experiment, because rapid movement of the ER in living cells otherwise provoked artefacts after photobleaching of CYP83A1-mCherry at a segment of the nuclear envelope. In four independent experiments, we observed a significantly

 © 2013 BSPP AND JOHN WILEY & SONS LTD

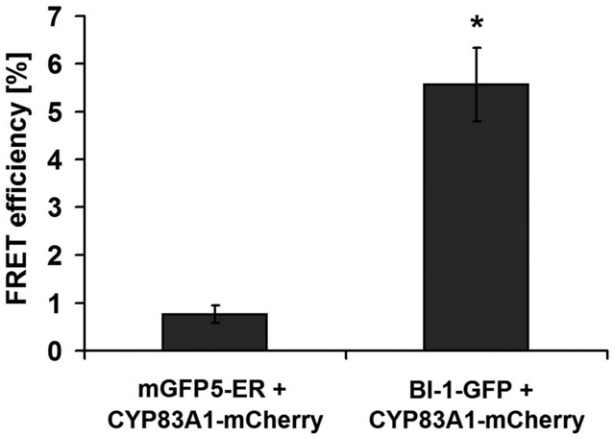

Fig. 4 BAX INHIBITOR-1 (BI-1) interacts with cytochrome P450 83A1 (CYP83A1) at the endoplasmic reticulum (ER). Quantitative measurement of fluorescence resonance energy transfer (FRET) after acceptor photobleaching using fixed *Arabidopsis* epidermal cells transiently co-expressing CYP83A1-mCherry and mGFP5-ER or BI-1-GFP. Columns represent the means of four independent experiments. In each experiment, 20 cells per variant were analysed. CYP83A1-mCherry, as the potential acceptor of FRET, was bleached at a segment of the nuclear envelope, and the fluorescence of BI-1-GFP, but not mGFP5-ER, increased locally. Bars represent standard errors; * indicates significance at $P < 0.05$ according to two-sided paired Student's *t*-test.

enhanced FRET efficiency in cells co-expressing BI-1-GFP and CYP83A1-mCherry relative to control cells expressing an ER-targeted GFP (mGFP5-ER; Haseloff *et al*., 1997; Siemering *et al*., 1996) together with CYP83A1-mCherry (Fig. 4). Co-IP, co-localization and FRET experiments thus suggest direct interaction of BI-1 and CYP83A1 at the ER.

DISCUSSION

In order to further elucidate the mode of action of BI-1 in plant–pathogen interactions and cell death suppression, we conducted a co-IP using BI-1-GFP-expressing *Arabidopsis* mutants. By this, we identified 95 putative BI-1-interacting proteins (Table S1).

In addition to the selected BI-1-interacting candidates analysed in this study, several other BI-1-GFP co-immunoprecipitated proteins are promising candidates for further investigations (Table S1). For instance, three importin β-like nuclear transport receptors, importin-α export receptor/protein transporter, TRANSPORTIN 1 and EXPORTIN 1, were BI-1-GFP co-immunoprecipitated. These proteins are particularly interesting in the light of the notion that the C-terminal sequence of the BI-1 protein is reminiscent of a nuclear targeting motif (Hückelhoven *et al*., 2003; Walter *et al*., 1994). Future investigation into the role of importin β-like nuclear transport receptors might elucidate a role of BI-1 in nuclear transport mechanisms, which constitute essential processes in plant defence signalling (Merkle, 2003; Wiermer *et al*., 2007).

PHB2 and RPN2—two putative BI-1 interactors

The *Arabidopsis PHB* family consists of seven genes (Van Aken *et al*., 2010). So far, diverse biological functions, such as the regulation of senescence, ethylene signalling, oxidative stress prevention and mitochondrial biogenesis, have been attributed to plant PHBs (Ahn *et al*., 2006; Chen *et al*., 2005; Christians and Larsen, 2007). In the present study, we found an *Arabidopsis phb2* mutant to be more sensitive to cell death-inducing toxin treatment. Localization studies revealed an accumulation of PHB2-RFP at the mitochondria (Fig. 3a, Fig. S5). Our co-IP data include further BI-1-GFP co-immunoprecipitated proteins, which are associated with mitochondria or chloroplasts (Table S1). Interestingly, mammalian BAX localized to plant mitochondria and induced the disintegration of mitochondria and chloroplasts, whereas *Arabidopsis* BI-1 can prevent BAX-induced organelle damage and cell death *in planta* (Kawai-Yamada *et al*., 2001; Yoshinaga *et al*., 2005). In yeast and mammals, tethering proteins have already been identified, which regulate the contact of the ER and mitochondria and their functional connection, for instance in the regulation of Ca^{2+} signalling-mediated apoptosis (De Brito and Scorrano, 2008; Hoppins *et al*., 2007; Iwasawa *et al*., 2011; Kornmann *et al*., 2009). The exact localization of PHB2 in plant mitochondria is not yet understood. The protein might be soluble or associated with the inner membrane. At the moment, we have no evidence for a direct physical interaction of BI-1 and PHB2. Therefore, we can only speculate on the role of PHB2 in stress-induced cell death suppression, possibly by interaction with BI-1 indirectly or after mitochondrial disintegration.

The ER-resident RPN2 protein and its potential role in the plant OST complex, and during plant–pathogen interactions, are not well characterized. Our approach also led to a co-precipitation of BI-1 with two further OST complex subunits, STAUROSPORIN AND TEMPERATURE SENSITIVE 3-LIKE A (STT3A, gi|115464937) and DEFECTIVE GLYCOSYLATION (DGL1, gi|14334506) (Table S1). OST complexes catalyse asparagine (N)-linked glycosylation, a protein modification reaction accompanied by correct protein folding, which is highly conserved amongst eukaryotes (Kelleher and Gilmore, 2006; Knauer and Lehle, 1999). This process is part of the cellular ER quality control, which aids in the monitoring of ER stress, and supports the appropriate modification of plant immune receptors (Eichmann and Schäfer, 2012; Kang *et al*., 2008; Koiwa *et al*., 2003; Liu and Howell, 2010; Saijo, 2010). Watanabe and Lam (2008) demonstrated a role of BI-1 in the suppression of ER stress-induced cell death. Because partial loss of RPN2 enhanced slightly the susceptibility to powdery mildew, functional RPN2 might act antagonistically to BI-1 or in the ripening of immune receptors acting in PAMP-triggered immunity. Further analyses are required to confirm a possible direct interaction of RPN2 and BI-1.

CYP83A1 interacts with BI-1 at the ER and is involved in cell death control and susceptibility to *E. cruciferarum*

CYP83A1 catalyses the initial conversion of aldoximes to thiohydroximates in the biosynthesis of glucosinolates. In this activity, CYP83A1 has high substrate specificity to methionine-derived aldoximes, the precursors of aliphatic glucosinolates (Bak *et al*., 2011; Bak and Feyereisen, 2001; Naur *et al*., 2003). Several hydrolysis products of glucosinolates, such as thiocyanates, nitrils or epithionitrils, play an important role in plant–herbivore interactions, either as deterrents or stimulants (Hopkins *et al*., 2009). However, the role of aliphatic glucosinolates in interactions of plants with fungal pathogens, especially during plant–powdery mildew interactions, is largely uncharacterized. We found a strong *E. cruciferarum* resistance phenotype on two independent *cyp83a1* mutants relative to wild-type plants (Fig. 1c,d). However, so far, we have no evidence for a functional connection of BI-1 and glucosinolate biosynthesis. Several CYP83 family members have been identified in plant species that do not belong to the order Capparales, and do therefore not accumulate glucosinolates, indicating a function of CYP83-like enzymes in other metabolic pathways (Bilodeau *et al*., 1999; Siminszky *et al*., 1999). Moreover, because of reduced sinapate ester and lignin syringyl monomer contents in *cyp83a1*/*ref2* mutants, a potential role of CYP83A1 in the phenylpropanoid pathway has been discussed (Hemm *et al*., 2003; Ruegger and Chapple, 2001). Adas *et al*. (1999) demonstrated a role of human CYP2E1, a homologue of CYP83A1, in the hydroxylation of free fatty acids, presumably as a process to maintain membrane integrity and therefore to control cell death, on stress stimuli. Interestingly, the hydroxylation activity increased in the presence of the electron transfer protein cytochrome b_5 (Adas *et al*., 1999). In *Arabidopsis*, Nagano *et al*. (2009) showed the interaction of BI-1 with fatty acid 2-hydroxylases (FAHs) via cytochrome b_5, which was suggested to be involved in cell death suppression. In mammals, BI-1 was shown to inhibit the production of reactive oxygen species (ROS) and resulting cell death by mediating the destabilization of the NADPH-dependent cytochrome P450 reductase (NPR)–CYP2E1 complex. BI-1 interacts with NPR and, to a lesser extent, with CYP2E1, which leads to a reduced electron transfer from NPR to CYP2E1, and thus reduced ROS production (Kim *et al*., 2009). Furthermore, the protein level of CYP2E1 might be regulated through BI-1-mediated enhancement of lysosomal activity (Lee *et al*., 2012). Whether similar processes occur in *Arabidopsis* plants is not yet clear. Future studies will focus on the potential role of CYP83A1 in the susceptibility to powdery mildew fungi and cell death suppression, and on the underlying molecular mechanisms.

In summary, our co-IP approach for the identification of BI-1-interacting proteins revealed a list of interesting candidates for further investigation. Some of the proteins analysed showed a function in BI-1-related processes, such as the regulation of the interaction with biotrophic powdery mildew and the regulation of cell death. Hence, the data constitute a basis for further elucidation of the mode of action of BI-1 and associated proteins.

EXPERIMENTAL PROCEDURES

Plants and growth conditions

Arabidopsis thaliana ecotype Col-0 was purchased from Lehle Seeds (Round Rock, TX, USA). The *BI-1-GFP*-expressing mutant, the empty Bin19 vector mutant (Kawai-Yamada *et al*., 2001), the *BI-1* knock-out mutant *atbi1-2* (Watanabe and Lam, 2006), the *cyp83a1* point mutant *ref2-1* (Hemm *et al*., 2003), which was renamed to *cyp83a1-2* here, and the marker line *mt-gk* (Nelson *et al*., 2007) have been described previously. *Arabidopsis* mutants with T-DNA insertions in At1g03860 (*PHB2*; SALK_004663C = *phb2-1* and SALK_061282C = *phb2-2*), At4g21150 (*RPN2*/*HAP6*; SALK_019955C = *rpn2-1* and SALK_017994C = *rpn2-2*), At4g13770 (*CYP83A1*; SALK_123405C = *cyp83a1-1*), At1g78900 (*VHA-A*; SALK_081473C and SALK_089595C) and At2g18960 (*AHA1*; SALK_065288C) were ordered from the Nottingham Arabidopsis Stock Centre (NASC), Nottingham, UK. Primers for semi-quantitative two-step RT-PCR-based expression analysis and confirmation of T-DNA insertions are listed in Tables S2 and S3, respectively (see Supporting Information). Gene models showing insert sites of T-DNA in *PHB2*, *RPN2* and *CYP83A1*, as well as the primer sites used in RT-PCR analysis, are displayed in Fig. S2. All *Arabidopsis* seeds were sown in a soil–sand mixture and stratified for 2 days at 4 °C before placement in a growth chamber at 22 °C, with a photoperiod of 10 h and 64% relative humidity. For *Agrobacterium tumefaciens*-mediated transient transformation of tobacco leaf segments, we used *N. tabacum* cv. Samsun. Tobacco plants were cultivated in a growth chamber at 18 °C, with a photoperiod of 16 h and a relative humidity of 65%.

Pathogens and inoculation

Erysiphe cruciferarum was maintained on Col-0 and on super-susceptible phytoalexin-deficient *pad4* mutants (Reuber *et al*., 1998). Plants were inoculated with a density of three to five conidia/mm^2, as described previously (Reitz *et al*., 2012). *Blumeria graminis* (DC) Speer f.sp. *hordei* was maintained on barley cv. Golden Promise in a growth chamber at 18 °C, with a photoperiod of 16 h and a relative humidity of 65%. Inoculation was performed by blowing spores off infected plants.

Co-IP assay

Four-week-old BI-1-GFP-expressing mutants, as well as control plants carrying the empty binary vector Bin19 (Kawai-Yamada *et al*., 2001), were either noninoculated or inoculated with approximately 80 conidia/mm^2 of *B. graminis* f.sp. *hordei* and 30 conidia/mm^2 of *E. cruciferarum*. Infected plants were harvested 12 h after inoculation together with noninoculated control plants. Total protein was extracted from 10 g of frozen plant material (a pool of each variant) using 10 mL of extraction buffer A [50 mM Tris-HCl, 150 mM NaCl, 1 tablet PhosStop® (Roche Deutschland Holding

GmbH, Grenzach-Wyhlen, Germany), 1% protease inhibitor cocktail (Sigma-Aldrich Chemie GmbH, Munich, Germany), 0.005% leupeptin, 100 μM sodium orthovanadate, 0.5% TritonX-100]. After 15 min of incubation on ice, the protein extract was diluted 1:1 with extraction buffer B (extraction buffer A without TritonX-100) and centrifuged for 10 min at 2900 ***g***. The supernatant was extruded through a 0.45-μm nylon filter. About 40 mg of protein extract (3 μg/μL) were incubated twice with 100 μL of prewashed (washing buffer A: 50 mM Tris-HCl, 100 mM NaCl, 0.05% TritonX-100) Protein A sepharose for 30 min on a rotor at 4 °C. The extract was added to previously washed GFP-Trap A® beads (ChromoTek, Munich, Germany; Rothbauer *et al*., 2008) and incubated on a rotor for 1 h at 4 °C. On centrifugation (700 ***g***, 20 s), the beads were washed twice in 12 mL of washing buffer A. Another washing step followed with the addition of 12 mL of washing buffer B (washing buffer A without TritonX-100). Samples were centrifuged again for 20 s at 700 ***g***, and the supernatant was replaced by 30 μL of NuPAGE® LDS Sample Buffer (4×; Invitrogen GmbH, Karlsruhe, Germany), together with 30 μL of 100 mM dithiothreitol (DTT). Incubation at 50 °C for 15 min reduced the disulphide bonds. Centrifugation (900 ***g***, 30 s) of the samples on MicroSpin™ columns (GE Healthcare, Little Chalfont, Buckinghamshire, UK) allowed the separation of the beads and precipitated proteins. For alkylation, 1:10 2-iodoacetamide (1 M) was added, and the samples were incubated for 30 min in the dark at room temperature.

Protein identification by LC-MS/MS

Nanoflow LC-MS/MS of tryptic peptides was performed on an amaZon ETD mass spectrometer (Bruker Daltronik, Bremen, Germany) coupled to an easy-nLC (Proxeon, Odense, Denmark). Peptides were separated on a self-packed 0.075 × 20-cm^2 reversed-phase column (Reposil, Dr. Maisch, Ammerbuch, Germany) using a 110-min gradient from 10% to 35% of buffer B (0.1% formic acid in acetonitrile) at a flow rate of 300 nL/min. Intact masses of eluting peptides were determined in enhanced scan mode, and the five most intense peaks were selected for further fragmentation by collision-induced dissociation (CID) and acquisition of fragment spectra in ultra-scan mode. Singly charged precursor ions, as well as ions with unknown charge state, were rejected. Dynamic exclusion was enabled and the dynamic exclusion duration was set to 10 s. Peaklist files were generated with DataAnalysis 4.0 (Bruker Daltonik, Bremen, Germany), and database searches were performed using the Mascot search engine version 2.3.01 (Matrix Science, London, UK) with a tolerance of 0.3 Da for peptide and 0.6 Da for fragment ions against the NCBI (http://.ncbi.nlm.nih.gov/) database (nr_20070216, 4 626 804 entries) and the viridiplantae subset of the NCBI database (339 709 entries), considering carbamidomethylation of cysteine residues (+57.01 Da) as a fixed modification and oxidation of methionine (+15.99 Da) and pyro-glutamic acid from Q or E (–18.01 Da) as variable modifications. The Mascot search result files were analysed using Scaffold version 2.6.2 (Proteome Software Inc., Portland, OR, USA). Threshold parameters were set as follows: protein probability, 80%; minimum number of peptides, 1; peptide probability, 80%. These parameters yielded a false-discovery rate of 8.8% at the protein level and 7.0% at the peptide–spectrum match level. Protein identifications of candidate proteins were further validated by manual inspection of the tandem mass spectra.

Staining methods

To analyse the number of *E. cruciferarum* produced conidiophores per colony, leaves were discoloured and stained with acetic ink, as described previously for the staining of epiphytic structures of *B. graminis* f.sp. *hordei* (Hückelhoven and Kogel, 1998).

Glucosinolate analysis by high-performance liquid chromatography (HPLC)

The measurement of the glucosinolate content of wild-type Col-0 and *cyp83a1* mutants was performed via HPLC/diode array detection (DAD) analysis according to Mikkelsen *et al*. (2003).

AAL toxin and heat shock treatment

For cell death induction, 10 μL of 100 μM AAL toxin (A8331, Sigma-Aldrich Chemie GmbH) solution were dropped on leaves of 5-week-old *Arabidopsis* plants. Distilled water served as a control. For heat stress experiments, 8-day-old seedlings, grown on half-strength Murashige and Skoog (MS) medium, were incubated at 35 °C for 3 h, followed by a 3-day recovery phase and an additional heat stress at 45 °C for 2 h.

Cloning of constructs for FRET experiments

For acceptor photobleaching FRET experiments, protein-coding sequences were cloned into the overexpression vector pGY-1 (Schweizer *et al*., 1999). To obtain pGY-1-BI-1-GFP, *BI-1-GFP* was amplified using gDNA of *BI-1-GFP*-expressing mutants (Kawai-Yamada *et al*., 2001) as template, and cloned directly into pGY-1. pGY-1-mGFP5-ER was obtained by subcloning *mGFP5-ER* from pBIN-mGFP5-ER (Haseloff *et al*., 1997; Siemering *et al*., 1996) into pGY-1. The genomic sequence of *CYP83A1* (At4g13770), lacking the stop codon, was isolated by PCR and cloned in frame with *mCherry* into pGY-1, resulting in pGY-1-CYP83A1-mCherry. The primers used are listed in Table S4 (see Supporting Information).

Cloning of constructs for co-localization studies in tobacco

For co-localization studies in tobacco, the respective protein-coding sequences were cloned into the modified binary vector pBI101+ (lacking the *β-glucuronidase* (*GUS*) coding sequence; Pröls and Roitsch, 2009). The *PHB2* (At1g03860) coding sequence was isolated by PCR and cloned in frame with *RFP* (AAS78495) into pGY-1, resulting in pGY-1-PHB2-RFP. The open reading frame of *RPN2* (At4g21150) was isolated by PCR and cloned in frame with *mCherry* into pGY-1, resulting in pGY-1-RPN2-mCherry. RFP, PHB2-RFP, BI-1-GFP, GFP, CYP83A1-mCherry and RPN2-mCherry expression cassettes were subcloned from pGY-1 into the internal *Hind*III site of modified pBI101+. All primers used are listed in Table S5 (see Supporting Information).

Co-localization studies in tobacco

Leaf segments of about 5-week-old tobacco plants were co-transformed with pBI101+-BI-1-GFP and pBI101+-RFP or pBI101+-PHB2-RFP, or were

co-transformed with pBI101+-BI-1-GFP or pBI101+-GFP, together with pBI101+-CYP83A1-mCherry or pBI101+-1-RPN2-mCherry, by agroinfiltration, as described by Yang *et al*. (2000).

Transformed leaf segments were analysed by confocal laser-scanning microscopy using the sequential scanning mode in order to avoid channel cross-talk. BI-1-GFP and GFP were excited by a 488-nm laser line and detected at 505–530 nm. RFP, PHB2-RFP, CYP83A1-mCherry and RPN2-mCherry were excited by a 561-nm laser line and detected at 580–650 nm.

FRET analysis

Arabidopsis epidermal cells were ballistically transformed with 1 μg per shot of pGY-1-BI-1-GFP or pGY-1-mGFP5-ER, together with 2 μg per shot of pGY-1-CYP83A1-mCherry, using a particle inflow gun, as described by Finer *et al*. (1992). To decrease ER movement, 24 h after bombardment, transformed leaves were fixed in 4% formaldehyde, as described previously by Opalski *et al*. (2005). Acceptor photobleaching FRET analysis was performed directly after fixation using the Leica Application Suite, Advanced Fluorescence 1.8.0 software (Leica Microsystems, Wetzlar, Germany). After imaging a cell co-expressing BI-1-GFP or mGFP5-ER, together with CYP83A1-mCherry, a defined region of interest at the nuclear envelope was bleached by five times scanning with the 561-nm laser line at 100% relative laser intensity (20% of 20-mW laser power at 561 nm). The cell was imaged again using the same settings as before bleaching. FRET efficiency in the bleached area was calculated from the donor fluorescence intensities before (D_{post}) and after (D_{pre}) bleaching as follows: $FRET_{eff} = (D_{post} - D_{pre})/D_{post}$. GFP was excited by a 488-nm laser line and detected at 505–530 nm. mCherry was excited by a 561-nm laser line and detected in the spectral range 580–650 nm.

Accession numbers

BAX INHIBITOR-1 (BI-1), At5g47120; cytochrome P450 83A1 (CYP83A1), At4g13770; RIBOPHORIN II (RPN2) family protein, At4g21150; PROHIBITIN 2 (PHB2), At1g03860; VACUOLAR ATP SYNTHASE SUBUNIT A (VHA-A), At1g78900; H^+-ATPASE 1 (AHA1), At2g18960.

ACKNOWLEDGEMENTS

We are grateful to Katharina Beckenbauer, Anna Livic and Constanze König for excellent technical support. We thank M. Kawai-Yamada (University of Tokyo, Japan) for providing BI-1-GFP-expressing and empty vector Bin19 *Arabidopsis* mutants, N. Watanabe (The State University of New Jersey, New Brunswick, NJ, USA) for providing the BI-1 knock-out mutant *atbi1-2*, and C. Chapple (Purdue University, West Lafayette, IN, USA) for providing the *ref2-1* mutant. We are grateful to J. Haseloff (University of Cambridge, UK) for providing pBIN-mGFP5-ER. We thank the Salk Institute Genomic Analysis Laboratory and the Nottingham Arabidopsis Stock Centre for generating and providing the sequence-indexed *Arabidopsis* T-DNA insertion mutants. This project was supported by a grant from the German Research Foundation (DFG) to R.E and R.H. (EI835/1), a DFG Heisenberg Fellowship to E.G. (GL346/5) and a DFG grant to E.I. (SFB924/A6).

REFERENCES

Adas, F., Salaün, J.P., Berthou, F., Picart, D., Simon, B. and Amet, Y. (1999) Requirement for omega and (omega;-1)-hydroxylations of fatty acids by human cytochromes P450 2E1 and 4A11. *J. Lipid Res.* **40**, 1990–1997.

Ahn, C.S., Lee, J.H., Reum Hwang, A., Kim, W.T. and Pai, H.S. (2006) Prohibitin is involved in mitochondrial biogenesis in plants. *Plant J.* **46**, 658–667.

Babaeizad, V., Imani, J., Kogel, K.H., Eichmann, R. and Hückelhoven, R. (2009) Over-expression of the cell death regulator BAX inhibitor-1 in barley confers reduced or enhanced susceptibility to distinct fungal pathogens. *Theor. Appl. Genet.* **118**, 455–463.

Bak, S. and Feyereisen, R. (2001) The involvement of two P450 enzymes, CYP83B1 and CYP83A1, in auxin homeostasis and glucosinolate biosynthesis. *Plant Physiol.* **127**, 108–118.

Bak, S., Beisson, F., Bishop, G., Hamberger, B., Höfer, R., Paquette, S. and Werck-Reichhart, D. (2011) Cytochromes P450. *Arabidopsis Book*, **9**, e0144.

Bilodeau, P., Udvardi, M.K., Peacock, W.J. and Dennis, E.S. (1999) A prolonged cold treatment-induced cytochrome P450 gene from *Arabidopsis thaliana*. *Plant Cell Environ.* **22**, 791–800.

Bolduc, N., Ouellet, M., Pitre, F. and Brisson, L.F. (2003) Molecular characterization of two plant BI-1 homologues which suppress Bax-induced apoptosis in human 293 cells. *Planta*, **216**, 377–386.

Carrara, G., Saraiva, N., Johnson, B.F., Gubser, C. and Smith, G.L. (2012) A six transmembrane topology for Golgi Anti-Apoptotic Protein (GAAP) and Bax Inhibitor 1 (BI-1) provides a model for the Transmembrane Bax Inhibitor Containing Motif (TMBIM) family. *J. Biol. Chem.* **287**, 15 896–15 905.

Chen, J.C., Jiang, C.Z. and Reid, M.S. (2005) Silencing a prohibitin alters plant development and senescence. *Plant J.* **44**, 16–24.

Chen, S., Glawischnig, E., Jørgensen, K., Naur, P., Jørgensen, B., Olsen, C.E., Hansen, C.H., Rasmussen, H., Pickett, J.A. and Halkier, B.A. (2003) CYP79F1 and CYP79F2 have distinct functions in the biosynthesis of aliphatic glucosinolates in *Arabidopsis*. *Plant J.* **33**, 923–937.

Christians, M.J. and Larsen, P.B. (2007) Mutational loss of the prohibitin AtPHB3 results in an extreme constitutive ethylene response phenotype coupled with partial loss of ethylene-inducible gene expression in *Arabidopsis* seedlings. *J. Exp. Bot.* **58**, 2237–2248.

Cowling, R.T. and Birnboim, H.C. (1998) Preliminary characterization of the protein encoded by human testis-enhanced gene transcript (TEGT). *Mol. Membr. Biol.* **15**, 177–187.

De Brito, O.M. and Scorrano, L. (2008) Mitofusin 2 tethers endoplasmic reticulum to mitochondria. *Nature*, **456**, 605–610.

Deshmukh, S., Hückelhoven, R., Schäfer, P., Imani, J., Sharma, M., Weiss, M., Waller, F. and Kogel, K.H. (2006) The root endophytic fungus *Piriformospora indica* requires host cell death for proliferation during mutualistic symbiosis with barley. *Proc. Natl. Acad. Sci. USA*, **103**, 18 450–18 457.

Dettmer, J., Schubert, D., Calvo-Weimar, O., Stierhof, Y.D., Schmidt, R. and Schumacher, K. (2005) Essential role of the V-ATPase in male gametophyte development. *Plant J.* **41**, 117–124.

Dettmer, J., Hong-Hermesdorf, A., Stierhof, Y.D. and Schumacher, K. (2006) Vacuolar H^+-ATPase activity is required for endocytic and secretory trafficking in *Arabidopsis*. *Plant Cell*, **18**, 715–730.

Di, C., Xu, W., Su, Z. and Yuan, J.S. (2010) Comparative genome analysis of PHB gene family reveals deep evolutionary origins and diverse gene function. *BMC Bioinformatics*, **11**, S22.

Dietz, K.J., Tavakoli, N., Kluge, C., Mimura, T., Sharma, S.S., Harris, G.C., Chardonnens, A.N. and Golldack, D. (2001) Significance of the V-type ATPase for the adaptation to stressful growth conditions and its regulation on the molecular and biochemical level. *J. Exp. Bot.* **52**, 1969–1980.

Eichmann, R. and Schäfer, P. (2012) The endoplasmic reticulum in plant immunity and cell death. *Front. Plant Sci.* **3**, 200. doi: 10.3389/fpls.2012.00200.

Eichmann, R., Dechert, C., Kogel, K.-H. and Hückelhoven, R. (2006) Transient over-expression of barley BAX Inhibitor-1 weakens oxidative defence and *MLA12*-mediated resistance to *Blumeria graminis* f.sp. *hordei*. *Mol. Plant Pathol.* **7**, 543–552.

Eichmann, R., Bischof, M., Weis, C., Shaw, J., Lacomme, C., Schweizer, P., Duchkov, D., Hensel, G., Kumlehn, J. and Hückelhoven, R. (2010) BAX INHIBITOR-1 is required for full susceptibility of barley to powdery mildew. *Mol. Plant–Microbe Interact.* **23**, 1217–1227.

Finer, J.J., Vain, P., Jones, M.W. and McMullen, M.D. (1992) Development of the particle inflow gun for DNA delivery to plant cells. *Plant Cell Rep.* **11**, 323–328.

Finni, C., Andersen, C.H., Borch, J., Gjetting, S., Christensen, A.B., de Boer, A.H., Thordal-Christensen, H. and Collinge, D.B. (2002) Do 14-3-3 proteins and plasma membrane H+-AtPases interact in the barley epidermis in response to the barley powdery mildew fungus? *Plant Mol. Biol.* **49**, 137–147.

Haseloff, J., Siemering, K.R., Prasher, D.C. and Hodge, S. (1997) Removal of a cryptic intron and subcellular localization of green fluorescent protein are required to

mark transgenic Arabidopsis plants brightly. *Proc. Natl. Acad. Sci. USA*, **94**, 2122–2127.

Hemm, M.R., Ruegger, M.O. and Chapple, C. (2003) The *Arabidopsis ref2* mutant is defective in the gene encoding CYP83A1 and shows both phenylpropanoid and glycosinolate phenotypes. *Plant Cell*, **15**, 179–194.

Hemrajani, C., Berger, C.N., Robinson, K.S., Marchès, O., Mousnier, A. and Frankel, G. (2010) NleH effectors interact with Bax inhibitor-1 to block apoptosis during enteropathogenic *Escherichia coli* infection. *Proc. Natl. Acad. Sci. USA*, **107**, 3129–3134.

Höfle, C., Loehrer, M., Schaffrath, U., Frank, M., Schultheiss, H. and Hückelhoven, R. (2009) Transgenic suppression of cell death limits penetration success of the soybean rust fungus *Phakopsora pachyrhizi* into epidermal cells of barley. *Phytopathology*, **99**, 220–226.

Hopkins, R.J., Van Dam, N.M. and Van Loon, J.J. (2009) Role of glucosinolates in insect–plant relationships and multitrophic interactions. *Annu. Rev. Entomol.* **54**, 57–83.

Hoppins, S., Lackner, L. and Nunnari, J. (2007) The machines that divide and fuse mitochondria. *Annu. Rev. Biochem.* **76**, 751–780.

Hückelhoven, R. (2004) BAX Inhibitor-1, an ancient cell death suppressor in animals and plants with prokaryotic relatives. *Apoptosis*, **9**, 299–307.

Hückelhoven, R. and Kogel, K.-H. (1998) Tissue-specific superoxide generation at interaction sites in resistant and susceptible near-isogenic barley lines attacked by the powdery mildew fungus (*Erysiphe graminis* f. sp. *hordei*). *Mol. Plant–Microbe Interact.* **11**, 292–300.

Hückelhoven, R., Dechert, C. and Kogel, K.-H. (2003) Overexpression of barley *BAX inhibitor 1* induces breakdown of *mlo*-mediated penetration resistance to *Blumeria graminis*. *Proc. Natl. Acad. Sci. USA*, **100**, 5555–5560.

Ihara-Ohori, Y., Nagano, M., Muto, S., Uchimiya, H. and Kawai-Yamada, M. (2007) Cell death suppressor *Arabidopsis* Bax Inhibitor-1 is associated with calmodulin binding and ion homeostasis. *Plant Physiol.* **143**, 650–660.

Imani, J., Baltruschat, H., Stein, E., Jia, G., Vogelsberg, J., Kogel, K.H. and Hückelhoven, R. (2006) Expression of barley BAX Inhibitor-1 in carrots confers resistance to *Botrytis cinerea*. *Mol. Plant Pathol.* **7**, 279–284.

Ishikawa, T., Watanabe, N., Nagano, M., Kawai-Yamada, M. and Lam, E. (2011) Bax inhibitor-1: a highly conserved endoplasmic reticulum-resident cell death suppressor. *Cell Death Differ.* **18**, 1271–1278.

Iwasawa, R., Mahul-Mellier, A.L., Datler, C., Pazarentzos, E. and Grimm, S. (2011) Fis1 and Bap31 bridge the mitochondria–ER interface to establish a platform for apoptosis induction. *EMBO J.* **30**, 556–568.

Johnson, M.A., von Besser, K., Zhou, Q., Smith, E., Aux, G., Patton, D., Levin, J.Z. and Preuss, D. (2004) *Arabidopsis* hapless mutations define essential gametophytic functions. *Genetics*, **168**, 971–982.

Kang, J.S., Frank, J., Kang, C.H., Kajiura, H., Vikram, M., Ueda, A., Kim, S., Bahk, J.D., Triplett, B., Fujiyama, K., Lee, S.Y., von Schaewen, A. and Koiwa, H. (2008) Salt tolerance of *Arabidopsis thaliana* requires maturation of N-glycosylated proteins in the Golgi apparatus. *Proc. Natl. Acad. Sci. USA*, **105**, 5933–5938.

Kawai, M., Panb, L., Reed, J.C. and Uchimiya, H. (1999) Evolutionally conserved plant homologue of the *Bax Inhibitor-1* (*BI-1*) gene capable of suppressing Bax-induced cell death in yeast. *FEBS Lett.* **464**, 143–147.

Kawai-Yamada, M., Jin, L., Yoshinaga, K., Hirata, A. and Uchimiya, H. (2001) Mammalian Bax-induced plant cell death can be down-regulated by overexpression of *Arabidopsis Bax Inhibitor-1* (*AtBI-1*). *Proc. Natl. Acad. Sci. USA*, **98**, 12 295–12 300.

Kawai-Yamada, M., Ohori, Y. and Uchimiya, H. (2004) Dissection of *Arabidopsis* Bax inhibitor-1 suppressing Bax-, hydrogen peroxide-, and salicylic acid-induced cell death. *Plant Cell*, **16**, 21–32.

Kawai-Yamada, M., Hori, Z., Ogawa, T., Ihara-Ohori, Y., Tamura, K., Nagano, M., Ishikawa, T. and Uchimiya, H. (2009) Loss of calmodulin binding to Bax inhibitor-1 affects *Pseudomonas*-mediated hypersensitive response-associated cell death in *Arabidopsis thaliana*. *J. Biol. Chem.* **284**, 27 998–28 003.

Keinath, N.F., Kierszniowska, S., Lorek, J., Bourdais, G., Kessler, S.A., Shimosato-Asano, H., Grossniklaus, U., Schulze, W.X., Robatzek, S. and Panstruga, R. (2010) PAMP (pathogen-associated molecular pattern)-induced changes in plasma membrane compartmentalization reveal novel components of plant immunity. *J. Biol. Chem.* **285**, 39 140–39 149.

Kelleher, D.J. and Gilmore, R. (2006) An evolving view of the eukaryotic oligosaccharyltransferase. *Glycobiology*, **16**, 47R–62R.

Kim, H.R., Lee, G.H., Cho, E.Y., Chae, S.W., Ahn, T. and Chae, H.J. (2009) Bax inhibitor 1 regulates ER-stress-induced ROS accumulation through the regulation of cytochrome P450 2E1. *J. Cell Sci.* **122**, 1126–1133.

Kiviluoto, S., Schneider, L., Luyten, T., Vervliet, T., Missiaen, L., De Smedt, H., Parys, J.B., Methner, A. and Bultynck, G. (2012) Bax Inhibitor-1 is a novel IP3 receptor-interacting and -sensitizing protein. *Cell Death Dis.* **3**, e367.

Knauer, R. and Lehle, L. (1999) The oligosaccharyltransferase complex from yeast. *Biochim. Biophys. Acta*, **1426**, 259–273.

Koiwa, H., Li, F., McCully, M.G., Mendoza, I., Koizumi, N., Manabe, Y., Nakagawa, Y., Zhu, J., Rus, A., Pardo, J.M., Bressan, R.A. and Hasegawa, P.M. (2003) The STT3a subunit isoform of the *Arabidopsis* oligosaccharyltransferase controls adaptive responses to salt/osmotic stress. *Plant Cell*, **15**, 2273–2284.

Kornmann, B., Currie, E., Collins, S.R., Schuldiner, M., Nunnari, J., Weissman, J.S. and Walter, P. (2009) An ER-mitochondria tethering complex revealed by a synthetic biology screen. *Science*, **325**, 477–481.

Lee, G.H., Ahn, T., Kim, D.S., Park, S.J., Lee, Y.C., Yoo, W.H., Jung, S.J., Yang, J.S., Kim, S., Muhlrad, A., Seo, Y.R., Chae1, S.W., Kim, H.R. and Chae, H.J. (2010) Bax inhibitor 1 increases cell adhesion through actin polymerization: involvement of calcium and actin binding. *Mol. Cell. Biol.* **30**, 1800–1813.

Lee, G.H., Kim, H.R. and Chae, H.J. (2012) Bax inhibitor-1 regulates the expression of P450 2E1 through enhanced lysosome activity. *Int. J. Biochem. Cell Biol.* **44**, 600–611.

Liu, J.X. and Howell, S.H. (2010) Endoplasmic reticulum protein quality control and its relationship to environmental stress responses in plants. *Plant Cell*, **22**, 2930–2942.

Merkle, T. (2003) Nucleo-cytoplasmic partitioning of proteins in plants: implications for the regulation of environmental and developmental signalling. *Curr. Genet.* **44**, 231–260.

Mikkelsen, M.D., Petersen, B.L., Glawischnig, E., Jensen, A.B., Andreasson, E. and Halkier, B.A. (2003) Modulation of *CYP79* genes and glucosinolate profiles in *Arabidopsis* by defense signaling pathways. *Plant Physiol.* **131**, 298–308.

Millar, A.H., Sweetlove, L.J., Giegé, P. and Leaver, C.J. (2001) Analysis of the *Arabidopsis* mitochondrial proteome. *Plant Physiol.* **127**, 1711–1727.

Nafisi, M., Sønderby, I.E., Hansen, B.G., Geu-Flores, F., Nour-Eldin, H.H., Nørholm, M.H.H., Jensen, N.B., Li, J. and Halkier, B. (2006) Cytochromes P450 in the biosynthesis of glucosinolates and indole alkaloids. *Phytochem. Rev.* **5**, 331–346.

Nagano, M., Ihara-Ohori, Y., Imai, H., Inada, N., Fujimoto, M., Tsutsumi, N., Uchimiya, H. and Kawai-Yamada, M. (2009) Functional association of cell death suppressor, *Arabidopsis* Bax inhibitor-1, with fatty acid 2-hydroxylation through cytochrome b. *Plant J.* **58**, 122–134.

Nagano, M., Takahara, K., Fujimoto, M., Tsutsumi, N., Uchimiya, H. and Kawai-Yamada, M. (2012) *Arabidopsis* sphingolipid fatty acid 2-hydroxylases (AtFAH1 and AtFAH2) are functionally differentiated in fatty acid 2-hydroxylation and stress responses. *Plant Physiol.* **159**, 1138–1148.

Naur, P., Petersen, B.L., Mikkelsen, M.D., Bak, S., Rasmussen, H., Olsen, C.E. and Halkier, B.A. (2003) CYP83A1 and CYP83B1, two nonredundant cytochrome P450 enzymes metabolizing oximes in the biosynthesis of glucosinolates in *Arabidopsis*. *Plant Physiol.* **133**, 63–72.

Nelson, B.K., Cai, X. and Nebenfuhr, A. (2007) A multicolored set of in vivo organelle markers for co-localization studies in *Arabidopsis* and other plants. *Plant J.* **51**, 1126–1136.

Nijtmans, L.G., de Jong, L., Artal Sanz, M., Coates, P.J., Berden, J.A., Back, J.W., Muijsers, A.O., Van der Spek, H. and Grivell, L. (2000) Prohibitins act as a membrane-bound chaperone for the stabilization of mitochondrial proteins. *EMBO J.* **19**, 2444–2451.

Opalski, K.S., Schultheiss, H., Kogel, K.-H. and Hückelhoven, R. (2005) The receptor-like MLO protein and the RAC/ROP family G-protein RACB modulate actin reorganization in barley attacked by the biotrophic powdery mildew fungus *Blumeria graminis* f.sp. *hordei*. *Plant J.* **41**, 291–303.

Pröls, R. and Roitsch, T. (2009) Extracellular invertase LIN6 of tomato: a pivotal enzyme for integration of metabolic, hormonal, and stress signals is regulated by a diurnal rhythm. *J. Exp. Bot.* **60**, 1555–1567.

Reintanz, B., Lehnen, M., Reichelt, M., Gershenzon, J., Kowalczyk, M., Sandberg, G., Godde, M., Uhl, R. and Palme, K. (2001) Bus, a Bushy *Arabidopsis cyp79f1* knockout mutant with abolished synthesis of short-chain aliphatic glucosinolates. *Plant Cell*, **13**, 351–367.

Reitz, M.U., Bissue, J.K., Zocher, K., Attard, A., Hückelhoven, R., Becker, K., Imani, J., Eichmann, R. and Schäfer, P. (2012) The subcellular localization of tubby-like proteins and participation in stress signaling and root colonization by the mutualist *Piriformospora indica*. *Plant Physiol.* **160**, 349–364.

Reuber, T.L., Plotnikova, J.M., Dewdney, J., Rogers, E.E., Wood, W. and Ausubel, F.M. (1998) Correlation of defense gene induction defects with powdery mildew susceptibility in *Arabidopsis* enhanced disease susceptibility mutants. *Plant J.* **16**, 473–485.

Robinson, K.S., Clements, A., Williams, A.C., Berger, C.N. and Frankel, G. (2011) Bax inhibitor 1 in apoptosis and disease. *Oncogene*, **30**, 2391–2400.
Rothbauer, U., Zolghadr, K., Muyldermans, S., Schepers, A., Cardoso, C.M. and Leonhardt, H. (2008) A versatile nanotrap for biochemical and functional studies with fluorescent fusion proteins. *Mol. Cell. Proteomics*, **7**, 282–289.
Ruegger, M. and Chapple, C. (2001) Mutations that reduce sinapoylmalate accumulation in *Arabidopsis thaliana* define loci with diverse roles in phenylpropanoid metabolism. *Genetics*, **159**, 1741–1749.
Saijo, Y. (2010) ER quality control of immune receptors and regulators in plants. *Cell. Microbiol.* **12**, 716–724.
Sanchez, P., De Torres Zabala, M. and Grant, M. (2000) AtBI-1, a plant homologue of Bax inhibitor-1, suppresses Bax-induced cell death in yeast and is rapidly upregulated during wounding and pathogen challenge. *Plant J.* **21**, 393–399.
Schuler, M.A. and Werck-Reichhart, D. (2003) Functional genomics of P450s. *Annu. Rev. Plant Biol.* **54**, 629–667.
Schweizer, P., Pokorny, J., Abderhalden, O. and Dudler, R. (1999) A transient assay system for the functional assessment of defense-related genes in wheat. *Mol. Plant–Microbe Interact.* **12**, 647–654.
Siemering, K.R., Golbik, R., Sever, R. and Haseloff, J. (1996) Mutations that suppress the thermosensitivity of green fluorescent protein. *Curr. Biol.* **6**, 1653–1663.
Siminszky, B., Corbin, F.T., Ward, E.R., Fleischmann, T.J. and Dewey, R.E. (1999) Expression of a soybean cytochrome P450 monooxygenase cDNA in yeast and tobacco enhances the metabolism of phenylurea herbicides. *Proc. Natl. Acad. Sci. USA*, **96**, 1750–1755.
Van Aken, O., Pecenkova, T., Van De Cotte, B., De Rycke, R., Eeckhout, D., Fromm, H., De Jaeger, G., Witters, E., Beemster, G.B., Inze, D. and Van Breusegem, F. (2007) Mitochondrial type-I prohibitins of *Arabidopsis thaliana* are required for supporting proficient meristem development. *Plant J.* **5**, 850–864.
Van Aken, O., Whelan, J. and Van Breusegem, F. (2010) Prohibitins: mitochondrial partners in development and stress response. *Trends Plant Sci.* **15**, 275–282.
Walter, L., Dirks, B., Rothermel, E., Heyens, M., Szpirer, C., Levan, G. and Gunther, E. (1994) A novel, conserved gene of the rat that is developmentally regulated in the testis. *Mamm. Genome*, **5**, 216–221.
Watanabe, N. and Lam, E. (2006) *Arabidopsis* Bax inhibitor-1 functions as an attenuator of biotic and abiotic types of cell death. *Plant J.* **45**, 884–894.
Watanabe, N. and Lam, E. (2008) BAX INHIBITOR-1 modulates endoplasmic reticulum stress-mediated programmed cell death in Arabidopsis. *J. Biol. Chem.* **283**, 3200–3210.
Wiermer, M., Palma, K., Zhang, Y. and Li, X. (2007) Should I stay or should I go? Nucleocytoplasmic trafficking in plant innate immunity. *Cell. Microbiol.* **9**, 1880–1890.
Xu, Q. and Reed, J.C. (1998) Bax Inhibitor-1, a mammalian apoptosis suppressor identified by functional screening in yeast. *Mol. Cell*, **1**, 337–346.
Yang, Y., Li, R. and Qi, M. (2000) In vivo analysis of plant promoters and transcription factors by agro infiltration of tobacco leaves. *Plant J.* **22**, 543–551.
Yoshinaga, K., Arimura, S., Hirata, A., Niwa, Y., Yun, D.J., Tsutsumi, N., Uchimiya, H. and Kawai-Yamada, M. (2005) Mammalian Bax initiates plant cell death through organelle destruction. *Plant Cell Rep.* **24**, 408–417.
Zhou, F., Andersen, C.H., Burhenne, K., Fischer, P.H., Collinge, D.B. and Thordal-Christensen, H. (2000) Proton extrusion is an essential signalling component in the HR of epidermal single cells in the barley–powdery mildew interaction. *Plant J.* **23**, 245–254.

SUPPORTING INFORMATION

Additional Supporting Information may be found in the online version of this article at the publisher's web-site:

Fig. S1 Co-immunoprecipitation of BAX INHIBITOR-1-green fluorescing protein (BI-1-GFP) and putative interacting proteins.
Fig. S2 Models of *PROHIBITIN* 2 (*PHB2*), *RIBOPHORIN II* (*RPN2*) and *cytochrome P450 83A1* (*CYP83A1*).
Fig. S3 Glucosinolate content of wild-type Col-0 and *cyp83a1-1*.
Fig. S4 Functional analysis of BAX INHIBITOR-1 (BI-1)-interacting candidate proteins in toxin response.
Fig. S5 Co-localization of PROHIBITIN 2-red/green fluorescing protein (PHB2-RFP/GFP)-labelled mitochondria.
Fig. S6 Co-localization of BAX INHIBITOR-1-green fluorescing protein (BI-1-GFP) and RIBOPHORIN II (RPN2)-mCherry or cytochrome P450 83A1 (CYP83A1)-mCherry at the endoplasmic reticulum.
Table S1 Proteins co-immunoprecipitated with BAX INHIBITOR-1-green fluorescing protein (BI-1-GFP) and identified by liquid chromatography and tandem mass spectrometry (LC-MS/MS).
Table S2 Oligo-DNA primers for the characterization of *prohibitin* 2 (*phb2*), *ribophorin II* (*rpn2*) and *cytochrome P450 83A1* (*cyp83a1*) mutants.
Table S3 Oligo-DNA primers used to confirm T-DNA insertion in *prohibitin* 2 (*phb2*), *ribophorin II* (*rpn2*) and *cytochrome P450 83A1* (*cyp83a1*) mutants.
Table S4 Oligo-DNA primers used for the cloning of fluorescence resonance energy transfer (FRET) constructs.
Table S5 Oligo-DNA primers used for the cloning of constructs for co-localization studies.